Kent Academic Repository

Title: The implications of thumb movements for Neanderthal and modern human manipulation

Authors: Ameline Bardo [1*], Marie-Hélène Moncel [2], Christopher J. Dunmore [1], Tracy L. Kivell[1,3], Emmanuelle Pouydebat [4], Raphaël Cornette [5]

[1] Skeletal Biology Research Centre, School of Anthropology and Conservation, University of Kent, Canterbury, Kent, CT2 7NR, United Kingdom.

[2] Département Homme et environnement, UMR7194–HNHP (CNRS – MNHN – UPVD – Sorbonne Universités), 1 rue René-Panhard, Paris, 75005, France.

[3] Department of Human Evolution, Max Planck Institute for Evolutionary Anthropology, D-04103 Leipzig, Germany.

[4] Département Adaptations du vivant, UMR 7179-CNRS/MNHN, MECADEV, Paris, 75321, France.

[5] Institut de Systématique, Évolution, Biodiversité, UMR 7205–CNRS/MNHN/UPMC/EPHE, National Museum of Natural History, 45 rue Buffon, Paris, 75005, France.

*Corresponding author: Dr. Ameline Bardo, A.Bardo-2183@kent.ac.uk

Abstract

Much research has debated the technological abilities of Neanderthals relative to those of early modern humans, with a particular focus on subtle differences in thumb morphology and how this may reflect differences in manipulative behaviors in these two species. Here, we provide a novel perspective on this debate through a 3D geometric morphometric analysis of shape covariation between the trapezial and proximal first metacarpal articular surfaces of Neanderthals (*Homo neanderthalensis*) in comparison to early and recent humans (*Homo sapiens*). Results show a distinct pattern of shape covariation in Neanderthals, consistent with more extended and adducted thumb postures that may reflect habitual use of grips commonly used for hafted tools. Both Neanderthals and recent humans demonstrate high intraspecific variation in shape covariation. This intraspecific variation is likely the result of genetic and/or developmental differences, but may also reflect, in part, differing functional requirements imposed by the use of varied tool-kits. These results underscore the importance of holistic joint shape analysis for understanding the functional capabilities and evolution of the modern human thumb.

Introduction

Variation in fossil hominin hand morphology has played a key role in the interpretation of how human manipulative abilities evolved [1-5]. There has been a particular focus on the thumb and the radial wrist bones, as their morphology is thought to reflect interspecific differences in the frequency and complexity of tool-related behaviors [2-15]. To better understand the morphological transitions that lead to the anatomically modern human (*Homo sapiens*) hand, many studies have analyzed how the human hand differs from that of Neanderthals (*Homo neanderthalensis*) [4, 11-13, 16]. Morpho-functional interpretations generally agree that both modern humans and Neanderthals were likely capable of the same dexterity [4, 17]. However, based on their robust phalanges, broader distal phalanges and joint configurations (see below), Neanderthal hands appear better adapted for forceful power grips that are considered important for the effective use of some tools, such as hafted Mousterian spears and scrapers [11, 13, 17-20]. However, a recent study by Karakostis and colleagues [16] argued that Neanderthal hand muscle attachment areas (entheses) are similar to those of recent humans that used precision grips throughout their professional life (e.g., tailors, shoemakers, joiners), suggesting the use of habitual precision, rather than power, grasping in Neanderthals. To better understand how Neanderthal and modern human thumb function may have varied, it is important to evaluate how the joints of the trapezium (including the first and second metacarpals, trapezoid and scaphoid facets) and the proximal joint of the first metacarpal (Mc1) correspond to each other. These joints are the primary osteological determinant of thumb mobility [21] and we refer to all of these joints together as the trapeziometacarpal (TMc) complex. Building on previous work [4, 11-12, 18], we investigate the morpho-functional characteristics of the thumb in Neanderthals, as well as early and recent modern humans, through a three-dimensional (3D)

geometric morphometric (GM) analysis [22] of shape covariation between the joints of the TMc

complex. This analysis of the entire trapeziometacarpal anatomical region is a more holistic

approach than in previous studies that have only focused on the trapezium-Mc1 articulation or

these bones in isolation [7-8, 10, 12, 14-15].

The morphological configuration of the thumb and radial side of the wrist is broadly

similar between the modern human and Neanderthal hands [5]. Compared with other great apes,

as well as some fossil hominins [23-24], modern humans and Neanderthals both show a broad,

relatively flat trapezial-metacarpal joint, including a palmarly-expanded trapezoid and an

extensive trapezium-scaphoid joint. Together, these features have been interpreted as

biomechanically advantageous for high loading from the thumb during frequent tool use and

production [3, 6-8]. However, the biomechanical implications of subtle morphological

differences between the TMc complexes of Neanderthals and modern humans have been less

clear [18]. Compared with modern humans, Neanderthals have a larger trapezial-Mc1 joint area

that is dorsopalmarly flatter [10, 12-13, 18]. This joint morphology has been interpreted as less

congruent and, therefore, possessing greater mobility that, in turn, would require greater

muscular force, or ligamentous support, than that of modern humans to achieve the same level of

joint stability [18]. Combined with other features of the hand, including robust phalanges, rugose

musculotendinous attachment sites, more parasagittally-oriented capitate-second metacarpal

facets, reduced third metacarpal styloid processes, radioulnarly flat fifth metacarpal bases, and

large, projecting carpal tubercles, this trapezial-Mc1 joint morphology has been interpreted as

evidence that power grips may have been more frequently used in the Neanderthal manipulative

repertoire than that of early modern humans [12, 19-20]. However, there is considerable

intraspecific variation in Neanderthal trapezial-Mc1 joint shape, and some specimens (e.g., La

79 Ferrassie 1) are difficult to distinguish from recent humans. Together with notable morphological

80 variation in the TMc complex morphology overall (e.g. Kebara 2) [19-20], this morphology

81 makes characterizing a 'typical' Neanderthal morphology challenging. An analysis of shape

82 covariation across the TMc complex may shed light on the subtle functional consequences of this

83 morphological variation within different Neanderthal individuals. Neanderthals had tool-kits

84 comprising diverse lithic types and sizes [25] that would require different hand grips to use [26],

85 but Neanderthals may also have practiced varied grasping behaviours due to differences in

86 geography [27], activities, time [28] and/or sex [29], all of which could be reflected within hand

87 morphology.

88   The shape variation found in previous studies in Neanderthals and modern humans [7-8,

89 10-15, 20], may be the result of multiple of factors, including genetics, evolutionary history,

90 hormones, sex, geography, and common developmental origin [30]. However, since bone

91 (re)models throughout life, it may also reflect, in part, variation in habitual use of the hand

92 during ontogeny. Although joint shape is commonly considered to be more genetically and

93 functionally constrained than other aspects of bone shape (e.g., shaft external or internal bone

94 structure) [31-32], within the hand, and in particular the small bones of the carpus, the

95 constraints on joint shape are less clear. The trapezium does not complete ossification in humans

96 until 9-10 years of age [33], while the base of the Mc1 does not completely fuse until 14-16.5

97 years of age. The trapezium develops within the hand surrounded by, and incurring load from,

98 five other bones. Further, both the trapezium and Mc1 will incur substantial muscular force,

99 directly or indirectly, from the intrinsic and extrinsic muscles of the radial side of the hand.

100 Strong and complex manipulative abilities are observed in modern humans before the end of the

101 total ossification of their carpal bones and the Mc1 [34]. Furthermore, Neanderthals are thought

102   to have made and used tools as juveniles [35]. As such, it is possible that frequent loading from

103   habitual manual activities during development and adulthood may subtly affect how the bones of

104   the TMc complex articulate with each other as their joint surfaces ossify. In this study, we assess

105   the morphological variation in the associated trapezia and first metacarpals of five Neanderthal

106   individuals (La Ferrassie 1 and 2, Le Régourdou 1, Kebara 2, Shanidar 4) and compare them to

107   five early modern humans (Qafzeh 9, Ohalo 2, Abri Pataud 26227 (AP-P1), Abri Pataud 26230

108   (AP-P3), Dame du Cavillon) as well as a broad sample of recent humans (Table 1, Fig. 1, and

109   Supplementary Information Table S1). Through a 3D GM approach using sliding semi-

110   landmarks [22], we analyze shape covariation across the joints of the TMc complex. While

111   previous analyses of 3D shape variation in the isolated trapezium, Mc1 or trapezoid have

112   revealed interspecific differences across hominins species [7-8, 14-15], the movement and

113   loading of the thumb is largely delimited by the interaction of the bones of the TMc complex

114   together. By analyzing shape covariation, we quantify, for the first time, how joint shapes vary

115   together across the trapezium and Mc1. That is, we explore how change in articular shape of

116   each articular facet is reflected in the shape of the remaining TMc complex facets. Just as the

117   functional interaction of the trapezial-Mc1 joint is the primary osteological determinant of thumb

118   mobility [21], we assume that all the functional joints of the two bones covary to some extent.

119   We aim to test the null hypothesis that joints of the TMc complex covary in the same way (i.e.,

120   same shape and relative orientations of the TMc joints) within Neanderthals, early modern and

121   recent modern humans, respectively. By quantifying the shape of all the joints of the TMc

122   complex together, we can holistically characterize its morphology in each species. This

123   characterization can elucidate which specific thumb movements and, by extension, which grip(s)

124   would have been favored by this morphology; that is, would each TMc complex be better suited

125   to precision (i.e., involvement of the pad of the fingers in opposition to the pad of the thumb) or

126   power grips (i.e., involvement of the palm of the hand).

127   Following previous studies of external and internal bone morphology, we predict that

128   humans will demonstrate a TMc complex morphology that favors thumb abduction [36-38] as

129   this movement, combined with axial pronation and flexion of the thumb, comprises thumb

130   opposition. An opposed thumb is habitually used by modern humans in strong precision "pad-to-

131   pad" grips [39], in which the thumb pad opposes the index finger pad, and the joints of the TMc

132   complex are oriented obliquely relative to the transverse plane. In contrast, we predict that

133   Neanderthals will show a morphology of the TMc complex favoring extended thumb

134   movements, associated with axially/parasagitally-oriented joints. This morphology is consistent

135   with habitual use of a transverse power squeeze grip, in which an object is held transversely

136   across the palm of the hand with strongly flexed fingers and the thumb is extended and adducted

137   to brace against the object [40]. This grip was used by humans when using hafted tools to scrape

138   wood in an experimental setting [41]. Thus, by studying the manner of shape covariation within

139   the TMc complex, we can infer the degree to which Neanderthals and modern humans shared

140   similar biomechanical advantages for high loading from a thumb held in different postures

141   during varied manipulative or tool-related behaviours [3, 6, 7-8].

142

143   **Results**

144   A multivariate regression of shape on centroid size tested for the size effects on

145   morphology. No allometric effect was found for either the trapezium or Mc1 indicating that the

146   size of bone alone cannot explain shape differences found between individuals and taxa

147   (Supplementary Information Table S2).

148   The 2B-PLS analysis showed that patterns of shape covariation between the joints of

149   trapezium and the Mc1 were significantly different between Neanderthals and recent humans

150   (Fig. 2A, C, and Table 2). Early modern humans showed no significant shape covariation

151   differences with either recent humans or Neanderthals (Table 2), and were always placed

152   intermediately in the PLS axes, presenting a shape covariation pattern between recent humans

153   and Neanderthals (Fig. 2). The 2B-PLS analysis revealed substantial intraspecific variation in

154   shape covariation for both recent humans and Neanderthals (Fig. 2).

155   The plot of the first PLS axis (PLS1) (33% of total covariance) separated Neanderthals

156   (positive values on PLS1 axis) from recent humans (negative values on PLS1 axis; Table 2), a

157   difference that was statistically significant. However, the Le Régourdou 1 Neanderthal fell

158   within the recent human morphological range of variation (Fig. 2A), and Qafzeh 9, the oldest

159   early modern human in our sample, fell within the Neanderthal morphological range of variation

160   (Fig. 2A). The range of PLS1 axis values reflected both differences in shape and relative joint

161   orientation, and these features did not vary in the same way within Neanderthals and within

162   modern humans. In recent modern humans (negative values on PLS1 axis), the joint surfaces of

163   both the trapezium and Mc1 were generally more curved and more obliquely-oriented relative to

164   the transverse plane, and the trapezial-Mc1 joint showed an extension of the radial border that

165   would be advantageous for more abducted, rather than adducted, thumb movements (Fig. 2A,

166   Fig. 3). In contrast, Neanderthals (positive values on PLS1 axis) showed joint surfaces of both

167   the trapezium and the Mc1 that were flatter and oriented closer to the transverse plane, with the

168   exception of the trapezial-Mc2 joint, which was oriented roughly parasagittally (Fig. 2A, Fig. 3).

169   The anteroposterior-flat and radioulnarly-convex shape of the Neanderthal trapezial-Mc1 joint is

170   radioulnarly wider and so more advantageous for a greater range of radio-ulnar, as well as

8

171 extended, thumb movements compared to recent modern humans (Fig. 2A, Fig. 3). Two

172 Neanderthal individuals fell out at opposite extremes (Fig. 2A); Le Régourdou 1 was the only

173 Neanderthal to fall within the modern human range of variation, while Kebara 2 was at the

174 extreme positive side of the axis, being most distinct from modern human shape covariation (Fig.

175 4).

176   The plot of PLS2 axis (28% of total covariance) revealed substantial overlap in shape

177 covariation between species, with all Neanderthals and all but two early modern human

178 individuals (Qafzeh 9 and AP-P3) falling within the range of variation seen in recent humans

179 (Fig. 2B). For individuals on the negative side of the PLS2 axis (including Neanderthals

180 specimens, La Ferrassie 1 and 2), the shape covariation was characterized by a posteroulnarly

181 extended articular surface of the trapezial-Mc1 joint, which could be more advantageous for

182 extended and adducted thumb movements. The trapezium joints were more obliquely-oriented

183 relative to the transverse plane, apart from the trapezial-Mc2 joint, which was oriented roughly

184 orthogonal to the transverse plane (Fig. 2B, Fig. 3). In contrast, individuals on the positive side

185 of the PLS2 axis (including Neanderthal specimens Kebara 2, Le Régourdou 1, Shanidar 4)

186 showed a posterioradially extended surface of the trapezial-Mc1 joint that could be advantageous

187 for extended and abducted thumb movements, and with joints more transversally-oriented (Fig.

188 2B and Fig. 3).

189   The plot of the PLS3 axis (14% of total covariance) showed overlap between taxa but

190 Neanderthals (positive values on PLS3 axis) were significantly different from recent humans

191 (negative values on PLS3 axis). Kebara 2 fell near the centre of the recent human distribution

192 and two recent humans fell within the Neanderthal distribution (Fig. 2C, Table 2). The PLS3 axis

193 showed high intraspecific variation in shape covariation of recent humans but also distinguished

194   western European Neanderthals (extreme positive values on PLS3 axis) from Near Eastern

195   Neanderthals, which were closer to the modern human distribution (Fig. 2C). The morphologies

196   reflected by PLS3 axis for western European Neanderthals and one recent human were quite

197   similar to those of the PLS2 axis: a flat and broad trapezial-Mc1 joint associated with an

198   anteroposteriorly thin ulnar portion of the trapezial-trapezoid joint, and joints more obliquely-

199   oriented relative to the transverse plane, apart from the trapezial-Mc2 joint, which was oriented

200   roughly orthogonal to the transverse plane (Fig. 2C). The trapezial-Mc1 joint showed extension

201   of the radial border that could be advantageous for abducted and extended movements of the

202   thumb (Fig. 2C, Fig.3). In contrast, the recent human specimens on the negative side of this axis

203   showed anteroposteriorly broad joints, a more anteroposteriorly-curved trapezial-Mc1 joint

204   obliquely-oriented relative to the transverse plane, a larger trapezial-trapezoid joint, and more

205   transversely-oriented trapezial joints (Fig. 2C). Furthermore, the shape of the trapezial-Mc1 joint

206   showed extension of the radial and ulnar border that would be advantageous for a greater range

207   of radioulnar movements of the thumb (Fig. 2C, Fig.3).

208

Discussion

210   We found significantly different patterns of shape covariation in Neanderthals and

211   modern humans on PLS axes that cumulatively comprise half of the total shape covariation (Fig.

212   2 A, C). These patterns demonstrate different shapes and relative joint orientations that suggest

213   contrasting patterns of habitual thumb movements and force transmission in Neanderthals and

214   modern humans.

215   The shape covariation patterns in early and recent modern humans support previous

216   studies; most joints are more obliquely-oriented relative to the transverse plane, which suggests a

217 biomechanical adaptation to the transmission of oblique force from the radial side of the hand [3,

218 6-8]. Thus, the general shape covariation pattern of the recent modern human TMc complex

219 would be advantageous for abducted thumb movements that would obliquely load the large

220 trapezial-trapezoid articular surface [6]. This human pattern is therefore also consistent with the

221 habitual use of forceful precision grips involving abduction of the thumb, such as during forceful

222 "pad-to-pad" precision grips [3, 39-40]. Interestingly, around half of modern humans have a

223 slightly different TMc complex morphology that could be more advantageous for adducted

224 thumb movements (Fig. 2 B, Fig. 3), which are used during oblique power squeeze gripping

225 (defined as an object held diagonally across the palm of the hand, clenched by flexed fingers and

226 buttressed by adducted thumb) [40], and powerful "pad-to-side" grip (handling of objects by the

227 thumb pad and the side of the index finger; *3*). These results are consistent with that of

228 Karakostis and colleagues [16] that found different hand bone entheseal patterns between

229 individuals known to engage in heavy manual work compared to precision workers. Thus, the

230 variation we found among modern humans may reflect different habitual manual activities across

231 our recent human sample.

232 In contrast to modern humans, most of the Neanderthals – though their intraspecific

233 variation is high – possess trapezial carpometacarpal joints that are more parallel to the

234 transverse plane while the trapezial-Mc2 joint is oriented parasagittally. Together, the joint

235 orientations of the Neanderthal TMc complex suggest a biomechanical adaptation to the

236 transmission of axial/parasagittal (i.e., parallel to the long axis of Mc1) force from the thumb

237 across the radial side of the hand [3, 7-8, 14]. The general shape covariation pattern would

238 facilitate an extended and adducted thumb during opposition of the thumb with the other fingers

239 in Neanderthals. This thumb posture suggests the habitual use of powerful transverse power

240 squeeze grips, like those used to grip hafted tools [12, 41]. The large axial loads generated by

241 this grip could be distributed across the joint surfaces provided by the more orthogonal/axial

242 orientation of the trapezial-Mc2 and trapezial-scaphoid joints in Neanderthals. The relatively

243 smaller trapezial-trapezoid joint surface on the Neanderthal trapezium also suggests that a greater

244 proportion of Mc1 load would be transmitted to the trapezium and the scaphoid. Conversely, the

245 large size of this joint in humans favours more force transmission across the anterior trapezoid to

246 the capitate during the power grip [6]. This pattern of shape covariation of Neanderthal TMc

247 morphology could have mechanically disadvantaged thumb abduction during grips such as

248 powerful "pad-to-pad" grip involving strong abduction, flexion and rotation of the thumb [3]

249 since more force would likely be transmitted through the smaller trapezial-trapezoid joint (Fig. 3-

250 4). However, we do not mean to suggest Neanderthals were incapable of the abducted hand

251 postures, but merely that their morphology made this less mechanically advantageous than in

252 modern humans. Indeed, Karakostis and colleagues [16] have shown that the same Neanderthals

253 specimens, apart Le Régourdou 1, possess an entheseal pattern consistent with this type of

254 precision grasping.

255 We cannot directly associate Neanderthal hand morphology with the specific lithic

256 assemblages as we do not know which individuals, or species in some cases, made or used these

257 artefacts. However, we know that late *Homo* species produced stone tools in this temporal and

258 geographical context. The different lithic technology and typology found, can inform us about

259 behavioural traditions occupying the region. Kebara 2 and Le Régourdou 1 showed the most

260 extreme differences in shape covariation among our Neanderthal sample (Fig. 2A, C). The

261 morphology of the TMc complex of Kebara 2 suggests mechanical advantage when loading a

262 more abducted thumb (Fig. 4), in agreement with current trabecular evidence [42], suggesting a

263 morphology favoring the use of "pad-to-pad" grips. This result is consistent with that of

264 Karakostis and colleagues [16] in which the Kebara 2 entheseal morphology suggests habitual

265 use of precision grips. Also, the Kebara 2 trapezium has a narrow and transversely-oriented Mc2

266 facet that brings it closer to the ulnar portion of the Mc1 facet. This particular morphology could

267 be disadvantageous to transmitting high load from the Mc2 to the trapezium during the adducted

268 thumb posture of powerful "pad-to-side" grips typically used with short and small flakes [26].

269 This is consistent with the Mousterian technology at Kebara where there are few retouched

270 flakes [27] and a greater abundance of longer flakes compared to Le Régourdou 1. Le Régourdou

271 1 is the only Neanderthal in our sample associated with Quina lithics, an industry with a high

272 proportion of scrapers [43], and smaller tools than those associated with Kebara 2. Le Régourdou

273 1 has a morphology advantageous for loading an adducted thumb, that this is used in a "pad-to-

274 side" grips used on scrapers. Therefore though it is only circumstantial evidence, it is interesting

275 that the two most disparate fossil Neanderthals in our sample appear to have morphologies that

276 would be mechanically advantageous for the grips associated with the type of tools frequently

277 found in techno complexes evidenced at the same site where these morphologies were found.

278   We found no significant differences in shape covariation between early modern humans

279 and Neanderthals, although sample sizes were small. The range of morphological variation found

280 in early modern humans was intermediate between that of recent modern humans and

281 Neanderthals. Interestingly, the closest early modern human to Neanderthals was Qafzeh 9, the

282 oldest individual in our sample at 95 ka [44] (Fig. 2A). Qafzeh hominins (found in Israel) and

283 Near Eastern Neanderthals existed during the same time period and both were found in

284 association with Middle Paleolithic industry, the Mousterian lithic technologies [44]. However,

285 previous analyses of the Qafzeh 9 hand morphology have interpreted this individual has likely

286 using finer and precise finger movements more often than Neanderthals [11], suggesting the use

287 of similar technology but with different manual abilities. The other early modern humans in our

288 sample, all younger than Qafzeh 9, were within the recent human range of morphological

289 variation, and are associated with a different technological context (i.e., including more blade

290 tools) than Qafzeh 9 [45-47].

291   To conclude, our results demonstrate that modern human and Neanderthal TMc complex

292 morphology does not covary in the same manner. Neanderthals possess trapezial

293 carpometacarpal joints that are flatter and more transversely oriented with extension of their

294 radial and ulnar borders, a trapezial-Mc2 joint that is orthogonal relative to the transverse plane,

295 and a small trapezial-trapezoid joint surface. All these features suggest transmission of axial

296 from the thumb across the radial side of the hand, favoring more extended and adducted thumb

297 movements during powerful opposition of the thumb with the other fingers. In support of shape

298 covariation reflecting habitual hand use, our results show that both Levantine and European

299 Neanderthals in our sample possess a thumb morphology suited for use in transverse power

300 squeeze grips on hafted tools. Although it should be noted that Shea [27] suggested that

301 Levantine Mousterians could have more frequently utilized hafted artefacts (e.g., spear points)

302 than European Mousterians. The morphology of Neanderthal hands analyzed here, would better

303 facilitate a type of force transmission through the wrist bones associated with the use hafted

304 tools, than that associated with non-hafted tools such as small flakes that require the use of "pad-

305 to-side" or "pad-to-pad" grips [3]. Comparing fossil morphology with contemporaneous lithic

306 industries can help us to infer past behavior and better understand the evolution of modern

307 human manipulative abilities.

308

309 **Materials and Methods**

310 **Materials**

311   The sample of recent modern humans comprises 40 adults with no sign of external

312 pathology from a broad geographic range (North America, Europe, Africa, North Asia;

313 Supplementary Information Table S1). As the fossil sample of early modern humans and

314 Neanderthals includes individuals of both or unknown sex and bones from both right and left

315 sides, our comparative human sample incorporated the same range of variation: 22 males, 15

316 females, three with no sex identified, and 25 bones (paired trapezium-Mc1) from the right side

317 and 15 from the left. Original fossils specimens were used for La Ferrassie 1 and 2, and we used

318 high-quality resin casts of the original specimens for Kebara 2, Le Régourdou 1 and Shanidar 4

319 (see Table 1 for additional information about these fossils). All the data were analyzed together

320 as neither sex nor side significantly affected shape covariation (Table 2).

321

322 **3D scanning**

323   Shape covariation of the Mc1 and trapezium were explored using 3D digital surface

324 models created from scan data collected via different methods including micro-computed

325 tomography (μCT), laser scanning (LS), and photogrammetry (P) (Supplementary Information

326 Table S1). The μCT scans of the samples were obtained as in Stephens et al. [37]. The 3D

327 models from μCT scans were constructed from TIFF data using Avizo 6.3 (FEI Visualization

328 Sciences Group, Hillsboro, USA) software. The LS scans were obtained with a NextEngine laser

329 scanner using a resolution of 28,000 points per square centimeter. Twelve scans were taken at

330 different positions on both side of the bone and then merged using the ScanStudio HD PRO

331 software. P scans were obtained using a Nikon D5100 DSLR camera with a resolution of 24

332 megapixels with a focal length was fixed to 55 mm (Objectif AF-S DX NIKKOR 18–55 mm VR

333 II) for all pictures. Fifty pictures were captured on both sides of the bone from different

334 viewpoints. For the reconstruction of the 3D models we used the Agisoft PhotoScan software

335 (2014 Agisoft LLC) obtaining a pixel size of 0.00490961 x 0.00490961 mm. Final meshes were

336 created using the Agisoft PhotoScan software with high values of 180000 optimal number of

337 polygons. Scanning artifacts or anomalies in the polygonal mesh, from all the µCt and LS

338 methods, were corrected using Geomagic Wrap 2015 (3D Systems, Inc) software. All imaging

339 data were analyzed together as there was no significant effect of acquisition method on shape

340 variation across species for either the trapezium joints or the Mc1 joint (MANOVA tests, $p >$

341 0.05). As we used right and left bones, we mirrored the left bones using Geomagic Wrap 2015

342 software, in order to ensure homologous comparisons.

343

3D geometric morphometrics

345   Because of the shape complexity of wrist bones and the challenges of identifying

346 homologous anatomical landmarks (i.e., point locations that are biologically homologous

347 between species) on irregularly-shaped joint surfaces, we quantified shape variation using a GM

348 approach with both 3D anatomical landmarks and 3D sliding semi-landmarks on curves and

349 surfaces [22]. 3D sliding semi-landmarks allow for the accurate description of anatomical zones

350 of high biological interest (like joint surfaces) even if the lack clear anatomical landmarks. 3D

351 sliding semi-landmarks on curves and surfaces correspond to Type III landmarks, in the typology

352 of Bookstein [48], which are geometric points dependent on the location of other landmarks.

353 Consequently, these semi-landmarks do not constitute absolute anatomical reference points and

354   so additional operations must be performed to be able to use them for shape comparisons (see

355   description of sliding procedure below).

356   Initially we created a landmark template for each bone by manually placing 3D

357   anatomical landmarks and 3D sliding semi-landmarks on curves and surfaces on one specimen

358   (Fig. 1, and Supplementary Information Figure S1 and Table S3), using Landmark [49]. Type II

359   3D anatomical landmarks [48] (five for the trapezium and two for the Mc1) were defined as

360   points of maximum curvature at the limits of joint surfaces on each specimen (described in

361   Supplementary Information Table S3). 3D curves were defined at the margins of articular

362   surfaces and were bordered by anatomical landmarks as recommended by Gunz *et al.* [50]. The

363   curves were digitized with a high density of points (62-142 points per curve depending on the

364   curve length) and then sub-sampled to the number listed in supplementary information

365   (Supplementary Information Table S3). A high density of 3D sliding semi-landmarks were

366   manually placed at approximately equidistant intervals on the entire surface of each bone (147

367   for all the joints of the trapezium and 41 for the proximal joint of first metacarpal). The template

368   used for the trapezium contains a total of 294 points including five anatomical landmarks, 142

369   semi-landmarks sliding on curves, and 147 semi-landmarks sliding on surfaces (Fig. 1 and

370   Supplementary Information Figure S1). The template used for the Mc1 contains a total of 105

371   points including two anatomical landmarks, 62 semi-landmarks sliding on curves and 41 semi-

372   landmarks sliding on surfaces (Fig. 1 and Supplementary Information Figure S1). To assess the

373   repeatability of the manual placement of the anatomical landmarks and curves for the trapezium

374   joints and the Mc1 proximal joint, we landmarked three similar Neanderthal specimens (same

375   sex, side and bone) ten times. Following a procrustes procedure, the first two principle

376   components of principle components analyses (PCA) revealed that shape variation among the

377   repetitions on each specimen tested was much lower than inter-specimen shape variation

378   (Supplementary Information Figure S2). Anatomical landmarks and curves for both bones were

379   thus considered repeatable.

380   The landmarking procedure continued by manually placing anatomical landmarks and

381   sliding semi-landmarks on curves on all the specimens, as was done for the templates. Next,

382   surface sliding semi-landmarks were projected onto each of the bone's surface [20] using the

383   function "placePatch" in the "Morpho" package [51] in R [52]. Then, the function "relaxLM" in

384   the "Morpho" package was used to relax landmark configuration onto each surface of both bones

385   (Mc1 and trapezium) by minimizing bending energy [51]. A sliding procedure was then

386   performed using the function "slider3d" in the "Morpho" package by minimizing the Procrustes

387   distance (see for details [20, 50]). After sliding, a general Procrustes analysis [53] was performed

388   for each specimen with the function "procSym" in the "Morpho" package, controlling for

389   differences in size, position and orientation of the bones between specimens. After this step, all

390   landmarks and sliding semi-landmarks can be analyzed as Procrustes 3D landmarks. Finally, the

391   size of each specimen, and for each bone separately, was quantified as centroid size (i.e. square

392   root of the summed of squared distances between each landmark and the center of gravity) [48]

393   in order to test for potentially confounding allometric effects on the study (see below).

394

395   **Statistical Analysis**

396   To reduce our large data set for statistical analysis, principle components analyses (PCA)

397   were performed using on the Procustes landmark sets using the function "procSym" in "Morpho"

398   package [51] on R. To investigate patterns of shape covariation between the trapezium and the

399   Mc1, Two-Block Partial Least-Squares (2B-PLS) analyses [54] were performed on the principle

400   component (PC) scores of each specimen with the "pls2B" function in the Morpho package [51].

401   By calculating a covariance matrix, 2B-PLS identifies axes that describe common shape

402   variation between the two bones (PLS axes) while reducing dimensionality of the dataset. To

403   visualize the co-varying morphology changes associated with the extremes of each PLS axes, the

404   "plsCoVar" function in "Morpho" was used [51]. To test for differences between the mean shape

405   covariation across the three groups (early modern humans, recent humans and Neanderthals)

406   omnibus one-way permutational MANOVAs (1000 permutations) were run on the Euclidean

407   distance matrices of the first three PLS axes scores (i.e. those that described more than 10% of

408   the total covariance). If these omnibus tests were significant, pairwise versions of the same test

409   were run to understand which groups were significantly different form each other. These

410   permutational MANOVA's were run using the "Vegan" [55] and "RVAideMemoire" [56]

411   packages with the "adonis" and "pairwise.perm.manova" functions, respectively. Before we

412   performed these tests, a test of multivariate homogeneity of variance was performed on the

413   Euclidean distance matrix that describes the PLS scores (function "betadisper" in the "Vegan"

414   package) and a Bonferroni correction was applied to all pairwise results, to ensure valid

415   comparisons (Table 2). Allometric effects on the results were tested using the function

416   "procD.lm" in the "geomorph" package [57].

417

418   **References**

419   1. Napier, J. R. Fossil hand bones from Olduvai Gorge. *Nature* **196**, 409-411 (1962).

420   2. Susman, R. L. Hand of Paranthropus robustus from Member 1, Swartkrans: fossil evidence for

421   tool behavior. *Science* **240**(4853), 781-784 (1988).

422   3. Marzke, M. W. Precision grips, hand morphology, and tools. *Am. J. Phys. Anthropol.* **102**, 91-

423   110 (1997).

424   4. Niewoehner, W. A., Bergstrom, A., Eichele, D., Zuroff, M., Clark, J. T. Digital analysis:

425   Manual dexterity in Neanderthals. *Nature* **422**, 395 (2003).

426   5. Tocheri, M. W., Orr, C. M., Jacofsky, M. C., Marzke, M. W. The evolutionary history of the

427   hominin hand since the last common ancestor of *Pan* and *Homo*. *J. Anat.* **212**, 544-562

428   (2008).

429   6. Lewis, O. J. The joints of the hand in *Functional Morphology of the Evolving Hand and Foot*

430   (ed. Lewis, O. J.) 89-115 (Oxford Univ. Press, 1989).

431   7. Tocheri, M. W. *et al.* Functional capabilities of modern and fossil hominid hands: Three-

432   dimensional analysis of trapezia. *Am. J. Phys. Anthropol.* **122**, 101-112 (2003).

433   8. Tocheri, M. W., Razdan, A., Williams, R. C., Marzke, M. W. A 3D quantitative comparison of

434   trapezium and trapezoid relative articular and nonarticular surface areas in modern humans

435   and great apes. *J. Hum. Evol.* **49**, 570-586 (2005).

436   9. Napier, J. R. The form and function of the carpo-metacarpal joint of the thumb. *J. Anat* **89**,

437   362 (1955).

438   10. Trinkaus, E. Olduvai Hominid 7 trapezial metacarpal 1 articular morphology: contrasts with

439   recent humans. *Am. J. Phys. Anthropol.* **80**, 411–416 (1989).

440   11. Niewoehner, W. A. Behavioral inferences from the Skhul/Qafzeh early modern human hand

441   remains. *Proc. Natl. Acad. Sci. U.S.A.* **98**, 2979–2984 (2001).

442   12. Niewoehner, W. A. A Geometric Morphometric Analysis of Late Pleistocene Human

443   Metacarpal 1 Base Shape in *Modern morphometrics in physical anthropology* (eds. Gunz, P.

444   Mitteroecker, P. Bookstein, F. L.) 285–298 (Springer, Boston, MA, 2005).

445   13. Niewoehner, W. A. Neanderthal hands in their proper perspective in *Neanderthals Revisited:*

446   *New Approaches and Perspectives* (eds. Harvati, K. and Harrison, T.) 157–190 (Springer,

447   2008).

448   14. Marzke, M. W. *et al.* Comparative 3D quantitative analyses of trapeziometacarpal joint

449   surface curvatures among living catarrhines and fossil hominins. *Am. J. Phys. Anthropol.* **141**,

450   38-51 (2010).

451   15. Marchi, D., Proctor, D. J., Huston, E., Nicholas, C. L., Fischer, F. Morphological correlates

452   of the first metacarpal proximal articular surface with manipulative capabilities in apes,

453   humans and South African early hominins. *Comptes Rendus Palevol* **16**, 645-654 (2017).

454   16. Karakostis, F. A., Hotz, G., Tourloukis, V., Harvati, K. Evidence for precision grasping in

455   Neandertal daily activities. *Sci. Adv.* **4**, eaat2369 (2018).

456   17. Churchill, S. E. Hand morphology, manipulation, and tool use in Neandertals and early

457   modern humans of the Near East. *Proc. Natl. Acad. Sci. U.S.A.* **98**, 2953–2955 (2001).

458   18. Villemeur, I. *La main des Néandertaliens : Comparaison avec la main des hommes de type*

459   *moderne morphologie et mécanique* (Paris : CNRS éditions, 1991).

460   19. Trinkaus, E. *The Shanidar Neanderthals* (Academic Press, 1983).

461   20. Trinkaus, E., Villemeur, I. Mechanical advantages of the Neanderthal thumb in flexion: a test

462   of an hypothesis. *Am. J. Phys. Anthropol.* **84**, 249-260 (1991).

463   21. Cooney, W. P., Lucca, M. J., Chao, E. Y. Linscheid, R. L. The kinesiology of the thumb

464   trapeziometacarpal joint. *J. Bone Jt. Surg. Am. Vol.* **63**, 1371-1381 (1981).

465   22. Gunz, P., Mitteroecker, P. Semilandmarks: a method for quantifying curves and surfaces.

466   *Hystrix* **24**, 103-109 (2013).

467   23. Bush, M. E., Lovejoy, C. O., Johanson, D. C., Coppens, Y. Hominid carpal, metacarpal, and

468   phalangeal bones recovered from the Hadar Formation: 1974–1977 collections. *Am. J. Phys.*

469   *Anthropol.* **57**(4), 651-677 (1982).

470   24. Kivell, T. L., Kibii, J. M., Churchill, S. E., Schmid, P., Berger, L. R. *Australopithecus sediba*

471   hand demonstrates mosaic evolution of locomotor and manipulative abilities. *Science*

472   **333**(6048), 1411-1417 (2011).

473   25. Moncel, M. H. *et al.* The Acheulean workshop of la Noira (France, 700 ka) in the European

474   technological context. *Quat. Int.* **393**, 112-136 (2016).

475   26. Key, A., Merritt, S. R., Kivell, T. L. Hand grip diversity and frequency during the use of

476   Lower Palaeolithic stone cutting-tools. *J. Hum. Evol.* **125**, 137-158 (2018).

477   27. Shea, J. J. A functional study of the lithic industries associated with hominid fossils in the

478   Kebara and Qafzeh caves, Israel in *The Human Revolution* (eds. Mellars P. A. and Stringer, C.

479   B.) 611–625 (Edinburgh Univ. Press, Edinburgh, 1989).

480   28. Vaquero, M. Introduction: neanderthal behavior and temporal resolution of archeological

481   assemblages in *High resolution archaeology and Neanderthal behavior* (ed. Carbonell . i

482   Roura, E.) 1-16 (Springer, Dordrecht, 2012).

483   29. Estalrrich, A., El Zaatari, S., Rosas, A. Dietary reconstruction of the El Sidrón Neandertal

484   familial group (Spain) in the context of other Neandertal and modern hunter-gatherer groups.

485   A molar microwear texture analysis. *J. Hum. Evol.* **104**, 13-22 (2017).

486   30. Klingenberg, C. P. Studying morphological integration and modularity at multiple levels:

487   concepts and analysis. *Phil. Trans. R. Soc. B.* **369**, 20130249 (2014).

488   31. Currey, J. D. *Bones: Structure and Mechanics* (Princeton Univ. Press, 2006).

489   32. Ruff, C., Holt, B., Trinkaus, E. Who's afraid of the big bad Wolff?: "Wolff's law" and bone

490   functional adaptation. *Am. J. Phys. Anthropol.* **129**(4), 484-498 (2006).

491   33. Scheuer, L., Black, S. The Upper Limb in *Developmental juvenile osteology* (eds.

492   Cunningham, C. Scheuer, L. Black, S.) 272-340 (Academic Press, 2000).

493   34. Exner, C. E. In-hand manipulation skills in *Development of hand skills in the child* (eds.

494   Case-Smith, J. and Pehoski, C.) 35-45 (Bethesda, MD: American Occupational Therapy

495   Association, 1992).

496   35. Spikins, P., Hitchens, G., Needham, A., Rutherford, H. The cradle of thought: growth,

497   learning, play and attachment in Neanderthal children. *Oxford J. Archaeol.* **33**(2), 111-134

498   (2014).

499   36. D'Agostino, P. *et al.* In vivo biomechanical behavior of the trapeziometacarpal joint in

500   healthy and osteoarthritic subjects. *Clin. Biomech.* **49**, 119-127 (2017).

501   37. Stephens, N. B., Kivell, T. L., Pahr, D. H., Hublin, J. J., Skinner, M. M. Trabecular bone

502   patterning across the human hand. *J. Hum. Evol.* **123**, 1-23 (2018).

503   38. Dunmore, C. J., Bardo, A., Skinner, M. M., Kivell, T. L. Trabecular variation in the first

504   metacarpal and manipulation in hominids. *Am. J. Phys. Anthropol.* **171**(2), 219-241 (2019).

505   39. Napier, J. R. The prehensile movements of the human hand. *J. Bone Jt. Surg. Br. Vol.* **38**(4),

506   902-913 (1956).

507   40. Marzke, M. W., Wullstein, K. L., Viegas, S. F. Evolution of the power ("squeeze") grip and

508   its morphological correlates in hominids. *Am. J. Phys. Anthropol.* **89**(3), 283-298 (1992).

509   41. Anderson-Gerfaud, P. Aspects of behaviour in the Middle Palaeolithic: functional analysis of

510   stone tools from southwest France in *The Emergence of Modern Humans: An Archaeological*

511   *Perspective* (ed. Mellars, P.) 389–418 (Edinburgh University Press, Edinburgh, 1990).

512   42. Dunmore, C. J. *et al.* The position of *Australopithecus sediba* within fossil hominin hand use

513   diversity. *Nat. Ecol. & Evol.* **4**, 911-918 (2020).

514   43. Delpech, F. L'environnement animal des Moustériens Quina du Périgord. *Paléo, Revue*

515   *d'Archéologie Préhistorique* **8**, 31-46 (1996).

516   44. Valladas, H. *et al.* Thermoluminescence dating of Mousterian Troto-Cro-Magnon'remains

517   from Israel and the origin of modern man. *Nature* **331**, 614-616 (1988).

518   45. Nadel, D., Hershkovitz, I. New subsistence data and human remains from the earliest

519   Levantine Epipalaeolithic. *Curr. Anthropol.* **32**, 631-635 (1991).

520   46. Villotte, S., Chiotti, L., Nespoulet, R., Henry-Gambier, D. Étude anthropologique des

521   vestiges humains récemment découverts issus de la couche 2 de l'abri Pataud (Les Eyzies-de-

522   Tayac-Sireuil, Dordogne, France). *Bull. Mém. Soc. Anthropol. Paris* **27**, 158–188 (2015).

523   47. Pinilla, B. *et al.* Usure dentaire et mode masticatoire de la Dame du Cavillon -Variabilité de

524   la nourriture des hommes modernes lors du dernier maximum glaciaire in *La grotte du*

525   *Cavillon sous la falaise des Baousse Rousse Grimaldi, Vintimille, Italie; Etude anatomique du*

526 *squelette de « la Dame du Cavillon* (ed. de Lumley, H.) 949-967 (CNRS éditions, Paris,

527 2016).

528 48. Bookstein, F. L. *Morphometric Tools for Landmark Data: Geometry and Biology*

529 (Cambridge University Press, New York, 1991).

530 49. Wiley, D. F., *et al. Evolutionary morphing*, Minneapolis, MN, USA, 23-28 Oct. 2005 (IEE

531 Computer Society, Minneapolis, 2005).

532 50. Gunz, P., Mitteroecker, P., Bookstein, F. L. Semilandmarks in Three Dimensions in *Modern*

533 *morphometrics in physical anthropology* (ed. Slice, D. E.) 73-98 (Springer, Boston, MA,

534 2005).

535 51. Schlager, S. Morpho and Rvcg – Shape Analysis in R in *Statistical Shape and Deformation*

536 *Analysis* (eds. Zheng, G., Li, S., Szekely, G.) 217-256 (Academic Press, 2017).

537 52. R Core Team R: *A language and environment for statistical computing*, R Foundation for

538 Statistical Computing (Vienna, Austria, 2016), https://www.R-project.org/.

539 53. Rohlf, F. J., Slice, D. Extensions of the Procrustes method for the optimal superimposition of

540 landmarks. *Syst. Biol.* **39**, 40-59 (1990).

541 54. Rohlf, F. J., Corti, M. Use of two-block partial least-squares to study covariation in shape.

542 *Syst. Biol.* **49**, 740-753 (2000).

543 55. Oksanen, J. *et al. Vegan, Community Ecology Package: Ordination, Diversity and*

544 *Dissimilarities* (R package version 2.4-4, 2018), https://cran.r-project.org

545 56. Hervé, M. *RVAideMemoire: Testing and Plotting Procedures for Biostatistics* (R package

546 version 0.9-75, 2020) https://CRAN.R-project.org/package=RVAideMemoire

547   57. Adams, D. C., Collyer, M. L., Kaliontzopoulou, A. *Geomorph: Software for geometric*

548   *morphometric analyses* (R package version 3.0.6., 2018), https://cran.r-

549   project.org/package=geomorph.

550   58. Guérin, G. *et al.* A multi-method luminescence dating of the Palaeolithic sequence of La

551   Ferrassie based on new excavations adjacent to the La Ferrassie 1 and 2 skeletons. *J.*

552   *Archaeol. Sci.* **58**, 147-166 (2015).

553   59. Howell, F. C. Evolutionary implications of altered perspectives on hominine demes and

554   populations in the later Pleistocene of western Eurasia in *Neandertals and modern humans in*

555   *Western Asia* (eds. Akazawa, T. Aoki, K. Bar-Yosef, O.) 5-27 (Springer, Boston, MA, 2002).

556   60. Meignen, L., Bar-Yosef, O. Kébara et le Paléolithique moyen du Mont Carmel (Israël).

557   *Paléorient* **14-2**, 123-130 (1988).

558   61. Halilaj, E. *et al.* In vivo kinematics of the thumb carpometacarpal joint during three isometric

559   functional tasks. *Clin. Orthop. Relat. Res.* **472**(4), 1114-1122 (2014).

560

576

Author contributions

578   A.B., M.-H. M., E.P., and R.C. conceived of and designed the study. A.B. collected and analyzed

579   the data. C.J.D. and R.C. contributed analysis tools. T.L.K. and M.-H. M. contributed data and

580   theoretical context. C.J.D. and T.L.K. contributed substantially to the interpretation of data. A.B.

581   wrote the manuscript with input from all authors.

582

Competing interests

584   The authors declare that they have no competing interests.

585

Data and materials availability

587   All data needed to evaluate the conclusions in the paper are present in the paper and/or the

588   Supplementary Information. Additional data related to this paper may be requested from the

589   authors.

Figure legends

591

592

Template of Mc1 and trapezium joint shape comparison.
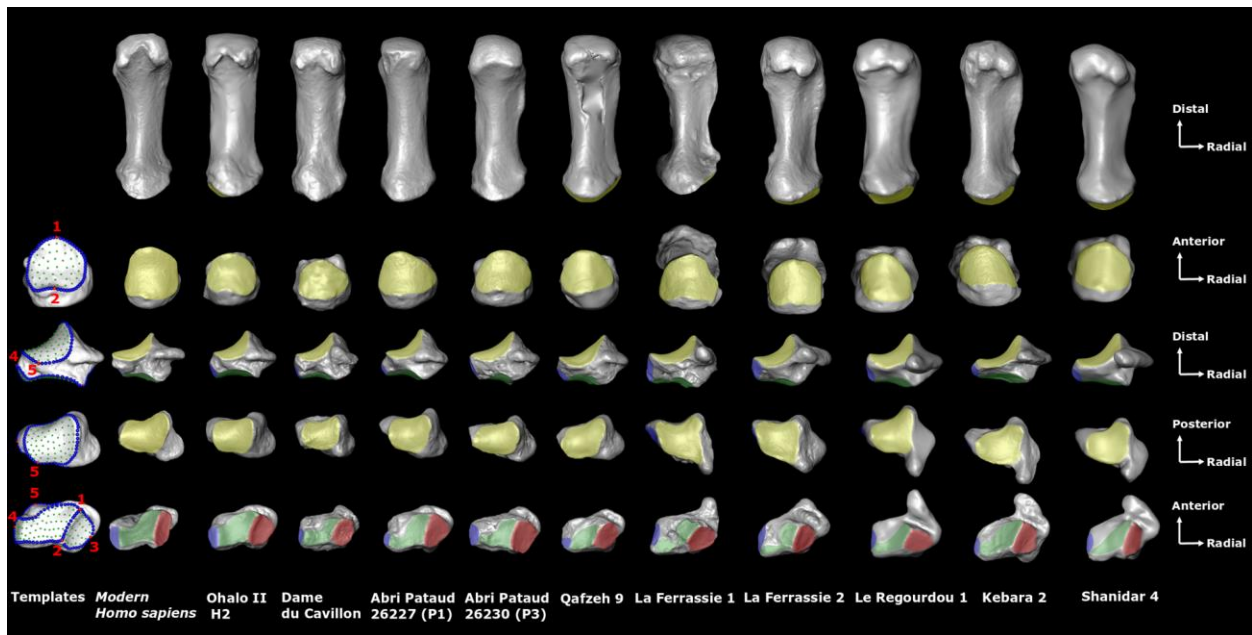
593 **Figure 1.** Joint shape comparison of the Mc1 (top 1st row, palmar view; top 2nd row, proximal

594 view) and trapezium (middle row, palmar view; 1st row from bottom, proximal view; 2nd row

595 from bottom, distal view) in modern human (2nd from left) and five early humans (3rd to 7th from

596 the left) and five Neanderthals (1st to 5th from right). Key colors: yellow, trapezial-Mc1 joint;

597 blue, 2nd metacarpal joint; green, trapezoid joint; red, scaphoid joint. The first column (left)

598 represents the landmark templates used in our analyses to quantify shape covariation (see

599 Materials and Methods, and detailed in Supplementary Information Figure S1 and Table S3).

600 The illustration is not scaled, and bones from the left-hand side (Le Régourdou 1, Kebara 2,

601 Shanidar 4, Abri Pataud P1, Abri Pataud P3, Dame du Cavillon) are mirrored for fair

602 comparison.

A 2B-PLS (33%)

Shapes associated to each extreme of the first PLS axis

B 2B-PLS (28%)

Shapes associated to each extreme of the second PLS axis

C 2B-PLS (14%)

Shapes associated to each extreme of the third PLS axis

603
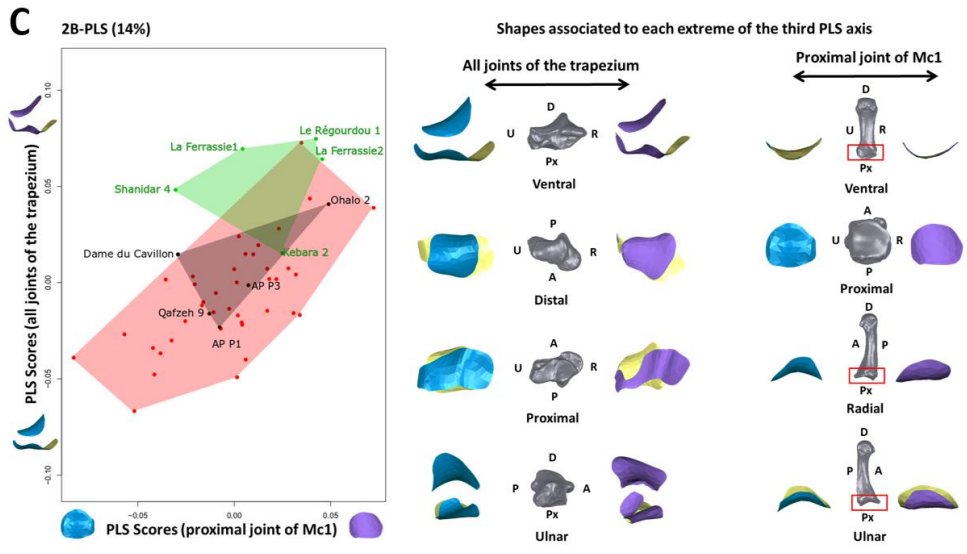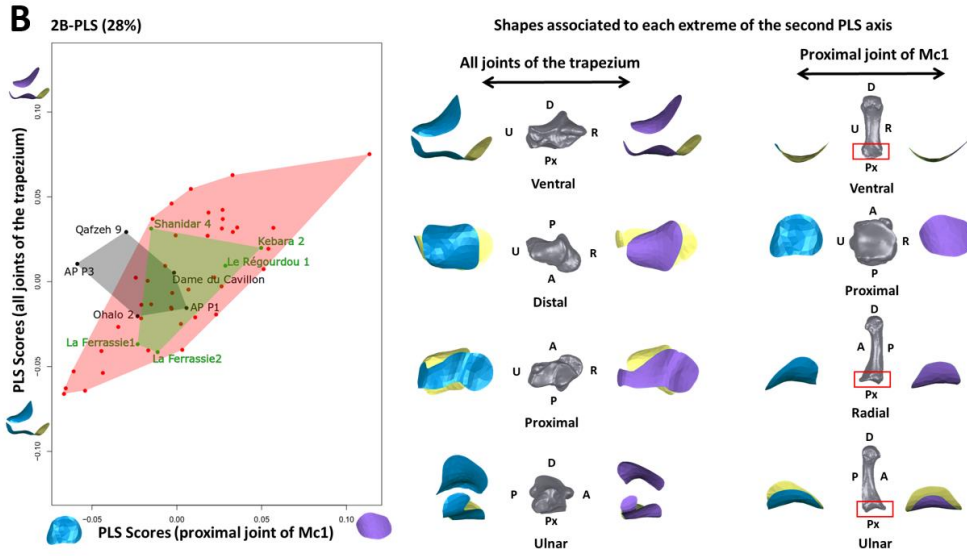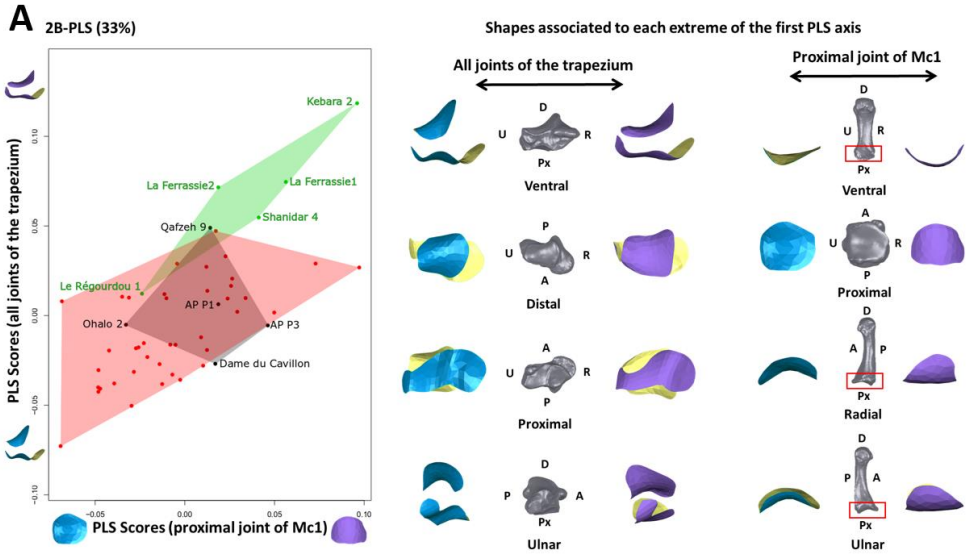
604   **Figure 2.** 2B-PLS of shape covariation between the proximal joint of Mc1 and all joints of the

605   trapezium across taxa. (**A**) 1st PLS axis; (**B**) 2nd PLS axis; (**C**) 3rd PLS axis. Neanderthals (green),

606   early modern humans (black) and modern humans (red). The figures on the right represent the

607   shapes associated with each minimum and maximum of the shape covariation axes (in blue and

608   purple, respectively) in different anatomical views (the full bone of a random *H. sapiens*

609   individual is depicted with each surface to aid interpretation). All shapes are scaled to

610   approximately the same length. A, anterior; P, posterior; D, distal; Px, proximal; R, radial; U,

611   ulnar.

612
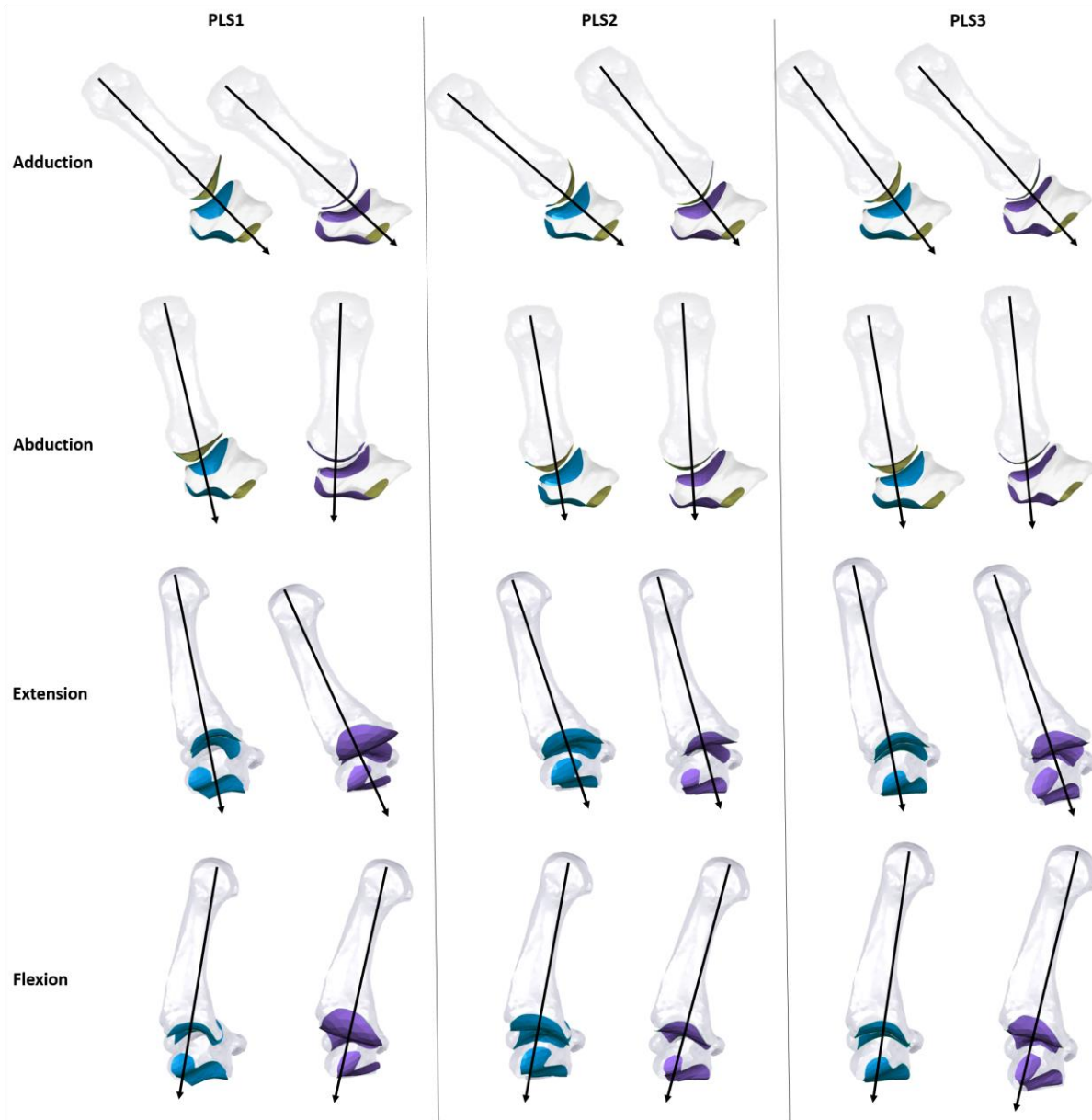
Figure 3. Illustration of possible movements of the TMc complex according to the shape

covariations associated with each positive (purple) and negative (blue) extremes of the first—

through-third PLS axes. For each shape configuration a direction of force transmission from the

Mc1 to the trapezium is suggested (black arrow). The illustration is not scaled.

613

614

615

616

617

618
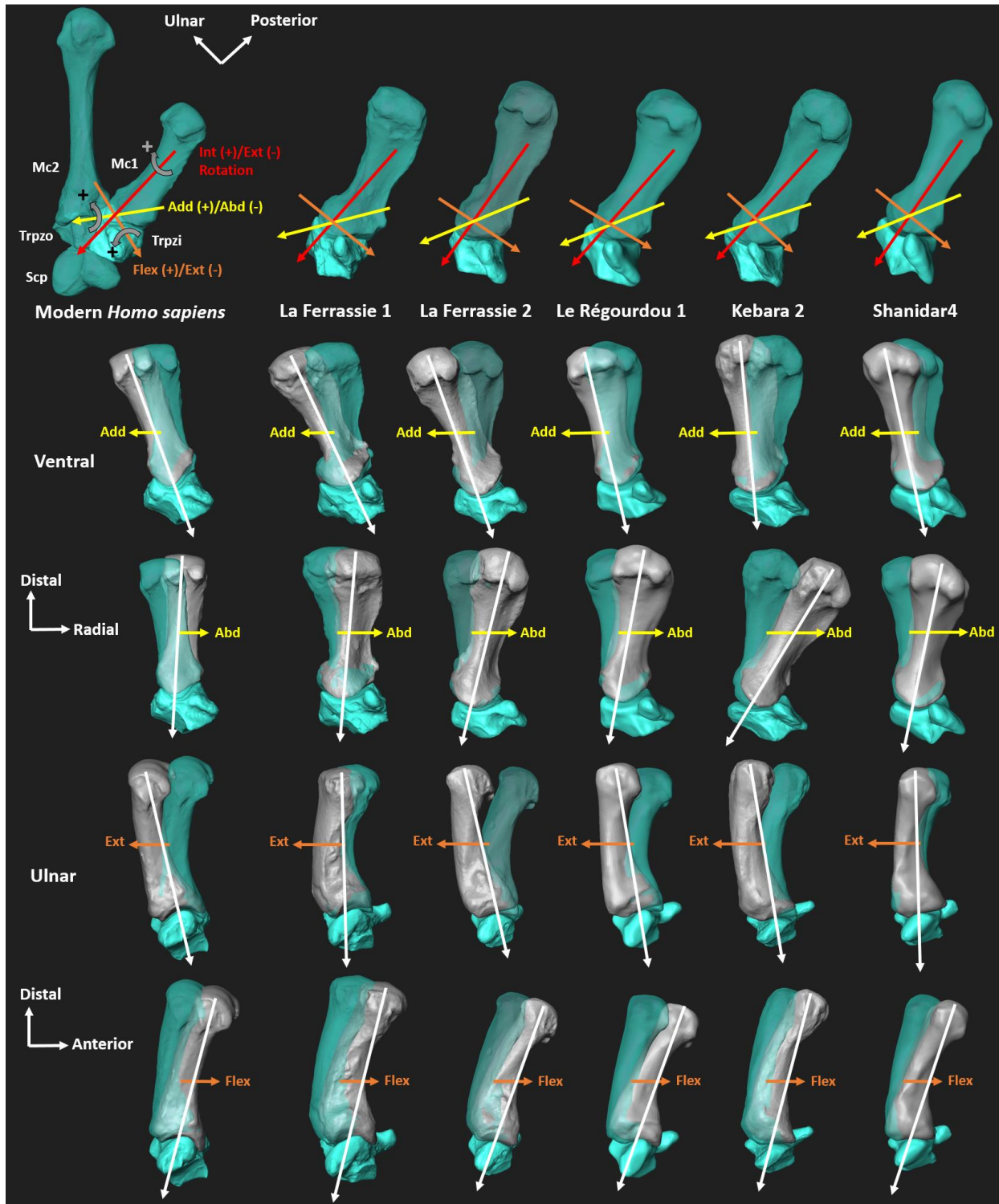
Figure 4. Illustration of potential TMc joint motion in the recent modern human (first column) and for the Neanderthal sample. The modern human specimen lies at the negative extreme end of the first PLS axis (Fig. 3A). This modern human specimen shows the other bones articulation

623   with the trapezium (Trpzi) and the first metacarpal (Mc1), the scaphoid (Scp), trapezoid (Trpzo)

624   and second metacarpal (Mc2). Each column corresponds to the suggested direction of trapezial-

625   Mc1 joint motion (following [61]) for one specimen. The bones are shown in neutral position

626   (grey) and in in motion (turquoise). Directions of motion are internal (Int +) and external (Ext -)

627   rotation (red), in adduction (Add +) and abduction (Abd -) (yellow), as well as flexion (Flex +)

628   and extension (Ext -) (orange). For each motion direction of force transmission from the Mc1 to

629   the trapezium is suggested based on the covarying morphology (white arrow). The trapezial-Mc1

630   joint is surrounded by a strong complex of ligaments and tendons [6, 33], which is not

631   considered in this illustration, as we don't have these soft tissues for fossils. Rotational

632   movements are not shown here. The illustration is not scaled.

Tables

634 **Table 1.** The fossil sample. [a] Casts; [b] I = indeterminate sex, n.b. the sex of Le Régourdou 1 is

635 still debated; [c] μCT = micro-computed tomography, LS = laser scanning, P = photogrammetry.

Species	Specimens	Date	Sex	Location	Cultural association	Acquisition methods[c]
Neanderthals	La Ferrassie 1	Middle Paleolithic - 43-45 ka [58]	M	France	Mousterian	P
	La Ferrassie 2	Middle Paleolithic - 43-45 ka [58]	F	France	Mousterian	P
	Le Régourdou 1[a]	Late Middle Paleolithic - 75 ka [43]	I[b]	France	Mousterian	LS
	Shanidar 4[a]	Middle Paleolithic - 46-54 ka [59]	M	Iraq	Mousterian	LS
	Kebara 2[a]	Middle Paleolithic - 43-50 ka [60]	M	Israel	Mousterian	P
Early modern humans	Qafzeh 9	Middle Paleolithic - 95 ka [44]	F	Israel	Mousterian	μCT
	Ohalo II H2	Early Upper Paleolithic - 19 ka [45]	M	Israel	Kebaran	μCT
	Abri Pataud 26227 (P1)	Early Upper Paleolithic – 26-28 ka [46]	F	France	"Proto-Magdalenian" (Gravettian)	P
	Abri Pataud 26230 (P3)	Early Upper Paleolithic – 26-28 ka [46]	F	France	"Proto-Magdalenian" (Gravettian)	P
	Dame du Cavillon	Early Upper Paleolithic - 24 ka [47]	F	France	Gravettian	P

636

637

638   **Table 2.** Results of omnibus and subsequent pairwise one-way permutational MANOVAs on the

639   first three PLS axes testing for differences in shape covariation between joints of trapezium and

640   proximal joint of the Mc1 across taxa, between the side of the bones (right and left) and sex.

641   Group multivariate variances were not significantly different ($p > 0.05$) and pairwise one-way

642   permutational MANOVAs were only carried out when omnibus permutational MANOVA tests

643   were significant. All values marked in bold where significant at $p < 0.05$, and are reported

644   subsequent to a Bonferroni correction.

645

	2B-PLS between all the joints of the trapezium and the Mc1 proximal joint		
	PLS1	**PLS2**	**PLS3**
All taxa	**< 0.0001**	0.6409	**0.0028**
Recent modern humans / Early modern humans	0.8895	-	1
Recent modern humans / Neanderthals	**0.0006**	-	**0.0012**
Neanderthals / Early modern humans	0.1464	-	0.1179
Side of the bones	0.0708	0.5351	0.6055
Sex	0.1404	0.2288	0.8324

646
647